



OPEN

Woody plant encroachment modifies carbonate bedrock: field evidence for enhanced weathering and permeability

Pedro A. M. Leite^{1✉}, Logan M. Schmidt^{2,3}, Daniella M. Rempe², Horia G. Olariu¹, John W. Walker⁴, Kevin J. McInnes⁵ & Bradford P. Wilcox¹

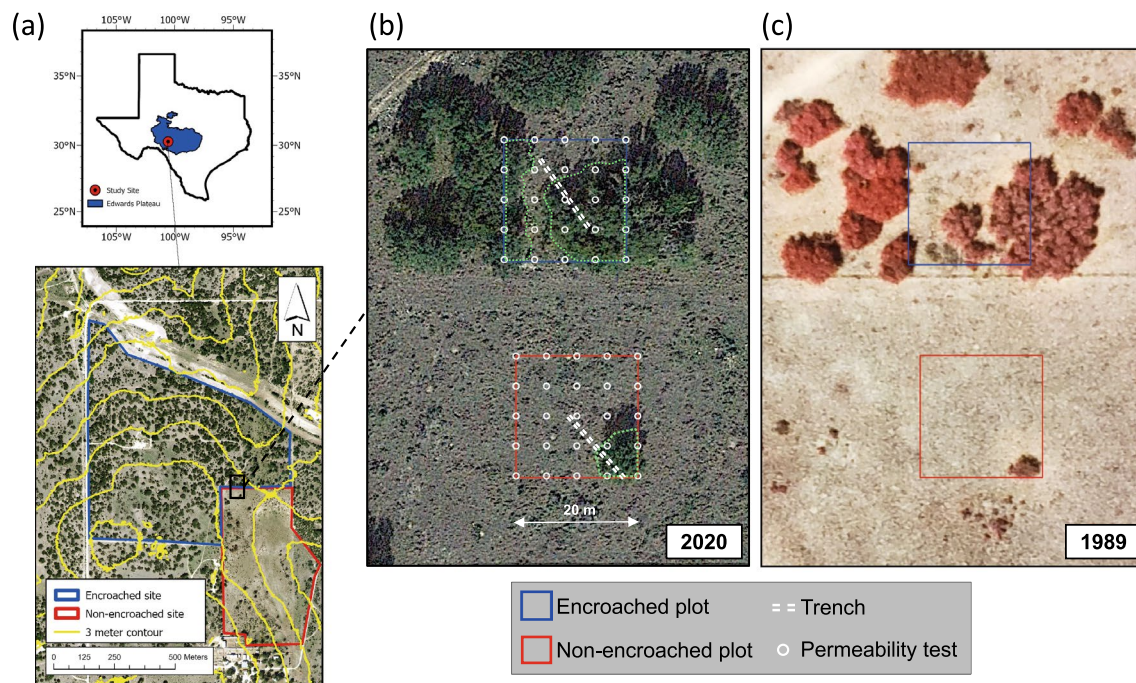
Little is known about the effects of woody plant encroachment—a recent but pervasive phenomenon—on the hydraulic properties of bedrock substrates. Recent work using stream solute concentrations paired with weathering models suggests that woody plant encroachment accelerates limestone weathering. In this field study, we evaluate this hypothesis by examining bedrock in the Edwards Plateau, an extensive karst landscape in Central Texas. We compared a site that has been heavily encroached by woody plants (mainly *Quercus fusiformis* and *Juniperus ashei*), with an adjacent site that has been maintained free of encroachment for the past eight decades. Both sites share the same bedrock, as confirmed by trenching, and originally had very few trees, which enabled us to evaluate how encroachment impacted the evolution of hydraulic properties over a period of no more than 80 years. Using *in situ* permeability tests in boreholes drilled into the weathered bedrock, we found that the mean saturated hydraulic conductivity of the bedrock was higher—by an order of magnitude—beneath woody plants than in the areas where woody plants have been continuously suppressed. Additionally, woody plant encroachment was associated with greater regolith thickness, greater plant rooting depths, significantly lower rock hardness, and a 24–44% increase in limestone matrix porosity. These findings are strong indicators that woody plant encroachment enhances bedrock weathering, thereby amplifying its permeability—a cycle of mutual reinforcement with the potential for substantial changes within a few decades. Given the importance of shallow bedrock for ecohydrological and biogeochemical processes, the broader impacts of woody plant encroachment on weathering rates and permeability warrant further investigation.

Woody plant encroachment (WPE) into grasslands and savannas, a land-cover change seen throughout the globe, has important implications for water and biogeochemical processes¹. Its effects on the water budget include changes in not only evapotranspiration, but also infiltration rates^{2,3}. Enhanced soil infiltrability following WPE has been demonstrated in many locations^{4–9} and can result in dramatic changes to both streamflow and groundwater recharge^{3,10,11}.

In some areas where soils are shallow, woody plants can utilize substantial amounts of rock moisture to sustain transpiration^{12–15}. As plants tap into bedrock, enhanced water and CO₂ fluxes along root channels may promote further rock dissolution, advancing weathering fronts and increasing bedrock permeability^{16–19}. This process creates a positive feedback mechanism that, over time, improves the bedrock's capacity to store moisture, making more water available to plants^{20–23}.

It has long been recognized that trees are important agents of biochemical and biomechanical weathering, but the spatial and temporal scales at which such weathering processes take place have seldom been addressed^{24,25}. Similarly, very little is known about the extent to which WPE—a relatively modern phenomenon—accelerates weathering of bedrock. Findings from recent studies suggest that WPE increases bedrock weathering and permeability. For example, in Kansas, increases in stream solute concentrations in limestone catchments have been

¹Department of Ecology and Conservation Biology, Texas A&M University, College Station, TX, USA. ²Department of Geological Sciences, Jackson School of Geosciences, University of Texas at Austin, Austin, TX, USA. ³Edwards Aquifer Authority, San Antonio, TX, USA. ⁴Texas A&M AgriLife Research and Extension Center, Texas A&M University, San Angelo, TX, USA. ⁵Department of Soil and Crop Sciences, Texas A&M University, College Station, TX, USA. ✉email: pedroleite@tamu.edu



Maps Data: Google Earth Engine @2020 USDA/ National Agriculture Imagery Program

Figure 1. (a) Location of our study sites within the Edwards Plateau of Texas and the experimental plots (black outline). (b) and (c) The experimental plots and immediate vicinity in 2020 (Google Earth image) and in 1989 (aerial imagery). In (b), white circles indicate points where bedrock permeability tests were performed and dashed lines indicate the locations of our trenches. Within the plots, dotted green lines delimit the zones covered by woody plants.

attributed to enhanced limestone weathering by WPE^{26–29}, although this hypothesis was not directly confirmed. In our study, we explored this hypothesis at two adjacent sites in the Edwards Plateau of Texas—one site long maintained mostly free of WPE and the other heavily encroached.

Study area

Our study took place between August 2020 and January 2021, at the Texas A&M Research Station near Sonora, TX, USA. The Station is located at approximately 700 m above sea level, in the southwestern portion of the Edwards Plateau—a major limestone formation that extends across much of West-Central Texas. Established for research purposes over 100 years ago, the 14-km² Sonora Station has been subject to diverse land uses and management practices over the years. The Station also houses detailed historical records of these uses and practices, making it an ideal location for comparative research. The climate is semiarid, with a mean annual temperature of 18 °C and mean annual precipitation of around 560 mm, 70% occurring as rainfall between May and October³⁰. Peak 15-min storm intensities of 90 mm/h have a return period of 2 years³¹.

The onset of WPE likely took place during the mid-1800s—in the wake of overgrazing and the suppression of natural fires—but it has accelerated in the last 60 years^{10, 32}. It is difficult to know the exact vegetation composition before European settlement and the introduction of livestock, but historical accounts suggest that this region was mostly covered with perennial grasses; woody plants occurred more sparsely, and denser stands were mainly associated with rock outcrops, escarpments, and waterways³². Available records show that from the 1890s until the 1960s the region was heavily overgrazed, with stocking rates more than ten times the current rates¹⁰.

The study area consists of a pair of sites: one site has undergone unrestrained encroachment by woody vegetation (encroached site), whereas the other has been continuously subjected to woody plant suppression since the 1940s (non-encroached site) (Fig. 1). Although the exact woody plant cover at the non-encroached site before the start of suppression is unknown, historical accounts for the Sonora Station suggest that very few trees were present. Until the 1970s, the suppression of woody plants at this site was carried out via sporadic mechanical removal, prescribed burns, and applications of herbicides, and since then by prescribed burns alone. In 1986, woody plant cover at the encroached and non-encroached sites was 7.6% and 5.4%, respectively, whereas by 2020 it was 19.3% and 4%, respectively (Figure S3). The dominant woody plant species at the encroached site are Ashe juniper (*Juniperus ashei*), Redberry juniper (*Juniperus pinchotii*), and Live oak (*Quercus fusiformis*). The few large woody plants at the non-encroached site consist mainly of scattered Live oak trees; a few small juniper saplings were also noted within the site. The intercanopy of both sites is largely dominated by a mixture of short and mid grasses and Prickly pear (*Opuntia spp.*). Both sites were grazed by sheep at high stocking rates from the late 1940s until the late 1960s. Since then, they have been grazed by sheep and goats at low stocking rates with periods of no grazing.

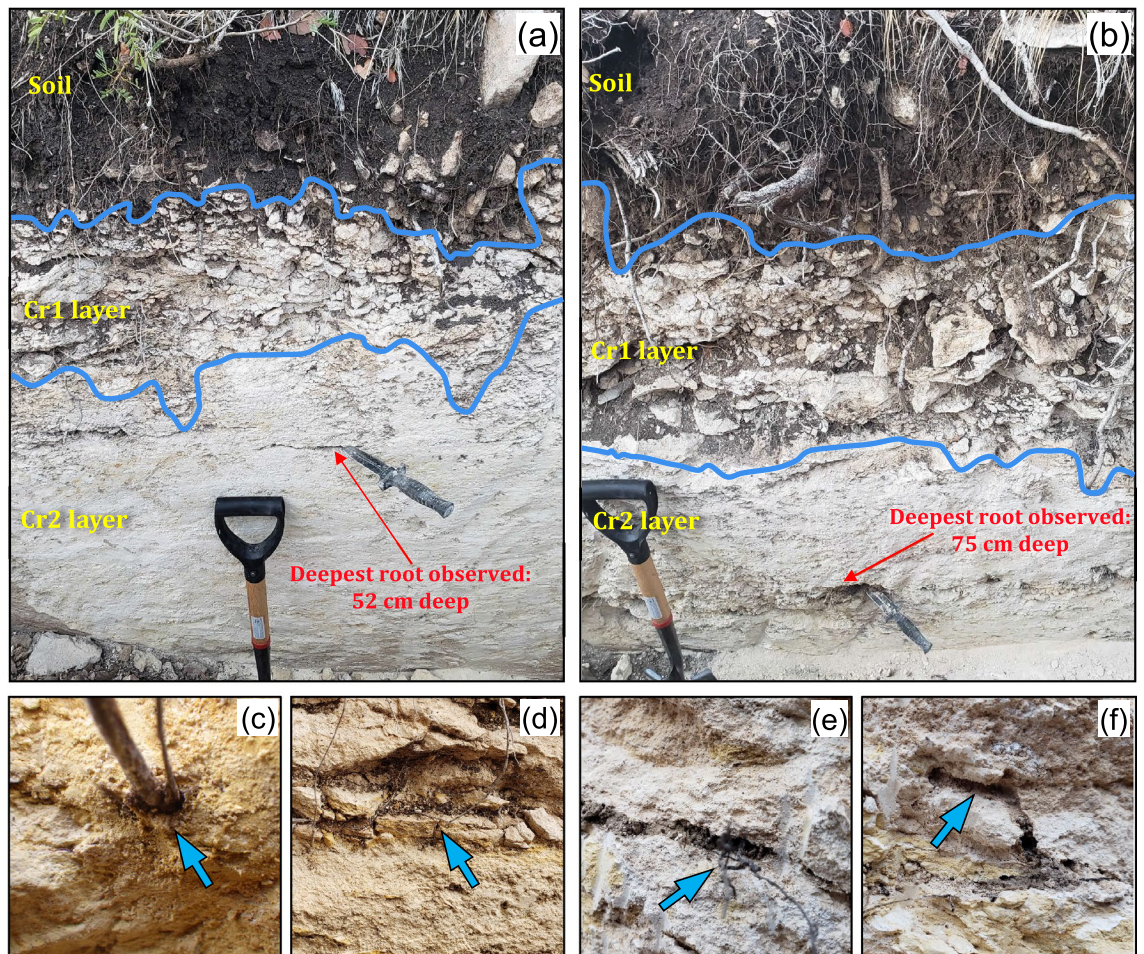


Figure 2. Profiles in the trench at the encroached site, at locations approximately 5 m apart and equally distant from the canopy dripline, in (a) an intercanopy zone and (b) a canopy zone. The knife is 20 cm long. (c) A 5-mm-thick root growing directly through the weathered limestone matrix. (d) Petrocalcic fragments between the Cr1 and Cr2 layers. (e) Wide fracture, filled with soil and woody roots, in the Cr2 layer. (f) Termite tunnels in the Cr2 layer.

The topographies of the two sites are comparable and range from level ground to very gentle slopes (< 3%). Both sites have very shallow soils (< 50 cm) and are underlain by the Buda formation (a 15- to 30-m-thick layer of Upper Cretaceous, fine-grained, bioclastic, and chalky limestone). The water table lies at depths greater than 50 m³³.

Within each site, we established a 20 m by 20 m experimental plot. These plots are 17 m distant from each other, are on near-level ground (no elevation differences between them), and are located on the same continuous bed. Both plots have a mixture of canopy and intercanopy cover (Fig. 1). The experimental plot within the encroached site (encroached plot) straddles two woody plant clusters separated by a narrow zone of intercanopy in the center and at the northern end. The plot within the non-encroached site (non-encroached plot) encloses mostly intercanopy cover with a single large Live oak tree in the southeast corner (Fig. 1). We determined that at the time of our study this oak tree was 54–57 years old, by counting the annual growth rings of a cross-section obtained from its main trunk (Figure S5). Woody plant cover on the plots and in their immediate vicinity was estimated (via the line intercept method) to be approximately 50% for the encroached plot and 4% for the non-encroached plot.

At both sites, we measured the permeability of shallow limestone bedrock in the canopy and intercanopy locations (*Methods*; Fig. 1) and excavated trenches (*Methods*; Figs. 1 and 2) to document root-zone properties (such as depth to the weathered bedrock, maximum rooting depth, rock hardness, and matrix porosity).

Results and discussion

Bedrock permeability is much higher under woody plants. Our results indicate that at both our study sites in the Edwards Plateau, WPE has significantly altered the hydraulic properties of the limestone bedrock. Two-way ANOVA results show that *cover* (canopy vs. intercanopy) was the only variable that had an effect on the mean saturated hydraulic conductivity (K_{sat} ; p -value = 0.001). Neither the *site* variable (non-encroached vs. encroached) nor the interaction term (*cover***site*) showed any effects (p -values > 0.7). Across both sites, the K_{sat} of the weathered bedrock was higher under woody plants (13 ± 18.6 mm/h) than in intercanopy zones

(1.17 ± 1.4 mm/h). K_{sat} under woody plants ranged between 0.12 and 64.7 mm/h), while in the intercanopy it ranged between 0.08 and 7.2 mm/h (Fig. 3a and Table S1).

Maps of interpolated K_{sat} values indicate that for both sites, areas of high K_{sat} broadly overlapped with the aerial extent of canopy cover (Fig. 3b). For the encroached site, K_{sat} values were highest near the center of the largest woody plant cluster and decreased sharply with proximity to the canopy/intercanopy boundaries (canopy dripline). Importantly, the fact that in the non-encroached site K_{sat} was substantially higher under the oak tree (which was less than 60 years old) suggests that enhancement of bedrock permeability by encroaching woody plants can occur in a few decades.

A plausible argument could be made that woody plants have established preferentially in areas where K_{sat} was already high. Some support for this alternative hypothesis is offered by studies showing that survival rates improve when seedlings establish in areas with bedrock heterogeneities such as fractures and weathered joints^{25, 34}. At the same time, other evidence suggests that woody plants are the main cause of the high K_{sat} values observed under their canopies. The fact that woody plant cover in the Edwards Plateau has been increasing continuously over the past few decades, reaching nearly 100% in some locations, by itself indicates that woody plant establishment is not necessarily predetermined by bedrock heterogeneities. Such heterogeneities are normally associated with topographic differences and bedding discontinuities^{35, 36}, which were not factors in our study: both plots have the same elevation, and both are located on the same continuous bed. If pre-existing bedrock heterogeneities were the cause of high permeability, more points with high K_{sat} values would be expected in the intercanopy of the non-encroached plot (where woody plants would likely be present had they not been continuously suppressed). In addition, the fact that K_{sat} was substantially higher under the woody plants in the eastern portion of the encroached plot than under those in the western portion (Fig. 3b) offers support for the hypothesis that trees can improve weathered bedrock permeability: the trees in the eastern portion are larger and older than those in the western portion, as shown by both aerial imagery from 1989 and our field survey (Fig. 1c and Figure S4). This observation suggests that—like soil infiltration capacity^{37, 38}—the effect of woody plants on limestone permeability can increase over time. Further investigations (e.g., including multiple sites representing chronosequences of WPE) could provide additional support to this hypothesis.

Other possible influences on bedrock permeability include the status (alive or dead), density, and species of woody plants. The eastern side of the encroached plot had several dead trees and higher tree density than the western portion (Figure S4). Greater density can mean more root biomass and higher competition for resources, which can drive trees to deepen their root profiles³⁹. Over time, as woody plants die and their roots

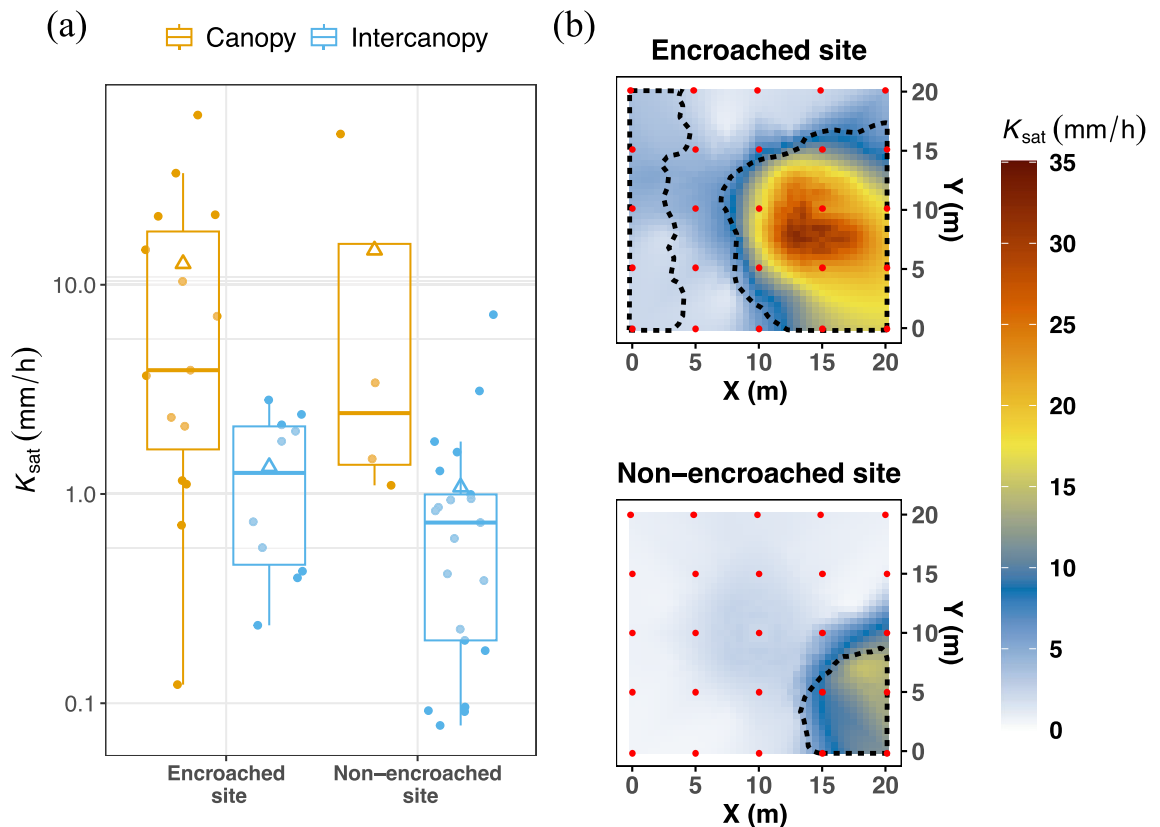


Figure 3. (a) Box plots showing the median, inter-quartile range, 95% confidence interval, and mean (triangles) of weathered bedrock K_{sat} in the canopy and intercanopy zones of the encroached and non-encroached sites. The y-axis was log₁₀-scaled for improved visualization. (b) Interpolation maps of K_{sat} for weathered bedrock in the encroached and non-encroached sites. The dotted black lines delimit the areas covered by woody plants and the red dots indicate the points at which the permeability tests were performed (see also Fig. 1b).

decay, preferential flow through root channels increases⁴⁰. Finally, the relatively low K_{sat} on the western side of the encroached plot may be due not only to the smaller size and younger age of the trees but also to their species: Ashe junipers (Figure S4) are known to have shallower rooting depths than Live oaks⁴¹. To clarify the roles of all these possible influencing factors, additional research is needed.

Mechanical and chemical weathering are enhanced under woody plants. While trees and shrubs have long been recognized as important agents of rock weathering and pedogenesis²⁴, very few studies have provided strong evidence of bedrock weathering as a result of WPE, or that such weathering can occur over short timescales. Woody plants can accelerate both mechanical weathering, via root growth and expansion into fractures (wedging), and chemical weathering, by increasing the concentration of reactive substances such as organic and inorganic acids⁴². Carbonate rocks such as limestone are particularly susceptible to chemical weathering by acids; the concentration of these acids can be increased by plants through root respiration and the addition of organic matter⁴³.

In our study, we found evidence that shallow bedrock properties were influenced by woody vegetation (Fig. 4 and Table S2). For soil thickness (i.e., depth to the Cr1 layer), there were no significant differences between sites ($p = 0.18$) or between cover types ($p = 0.91$). However, for regolith thickness (i.e., depth to the Cr2 layer) while there were also no significant differences between sites ($p = 0.24$), there was a significant difference between cover types ($p < 0.001$): the mean regolith thickness in the canopy zones was 59 ± 7.8 cm for the encroached site and 49.7 ± 7.2 cm for the non-encroached site).

With respect to the maximum observed rooting depths, both the *site* and *cover* variables had significant effects ($p < 0.001$): the highest mean value was found for canopy cover in the encroached site (80.1 ± 20.6), and the lowest mean value was found for intercanopy cover in the non-encroached site (46.6 ± 11.2) (Fig. 4 and Table S2). No significant effects were found for interactions between the variables *site* and *cover*.

Our analysis of limestone samples showed that matrix porosity ranged between 0.2 and 0.51 $\text{cm}^3\text{cm}^{-3}$ for the Cr1 layer and between 0.26 and 0.52 $\text{cm}^3\text{cm}^{-3}$ for the Cr2 layer. For the Cr1 layer, median porosity was 0.44 $\text{cm}^3\text{cm}^{-3}$ in both the canopy and intercanopy zones of the encroached site and in the canopy zone of the non-encroached site, but was significantly lower (0.31 $\text{cm}^3\text{cm}^{-3}$; $p < 0.001$) in the intercanopy zone of the non-encroached site (Fig. 5 and Table S2). For the Cr2 layer, median porosity values were highest in the encroached site, with no significant differences between canopy (0.45 $\text{cm}^3\text{cm}^{-3}$) and intercanopy (0.47 $\text{cm}^3\text{cm}^{-3}$) zones. For the non-encroached site, the median porosity of the canopy zone (0.41 $\text{cm}^3\text{cm}^{-3}$) was not statistically different ($p = 0.11$) from that of the intercanopy zones (0.33 $\text{cm}^3\text{cm}^{-3}$), but the intercanopy median porosity was significantly lower ($p = 0.015$) than that of the encroached site (Fig. 5).

For both sites, the median rebound (R) values (a proxy for rock hardness; these values are unitless and have a range of 10 to 100) for the Cr1 layer were significantly lower ($p < 0.01$) in canopy than in intercanopy zones (11.6 vs. 18.6 at the encroached site and 20.4 vs. 32.2 at the non-encroached site). Same-cover comparisons between the two sites showed significantly lower median R values for the encroached site ($p < 0.01$). Further, median R values for the Cr2 layer at the encroached site were similar for canopy and intercanopy zones (12 and 12.6) but were significantly different ($p < 0.01$) at the non-encroached site: 14.7 in the canopy zone versus 23.8 in the intercanopy zone. Rebound values and matrix porosity were inversely correlated ($p < 0.001$, $R^2 = 0.65$; Figure S7).

Under the assumptions that (1) porosity across both sites was comparable before woody plant suppression started in the early 1940s, and (2) the documented differences in matrix porosity are primarily attributable to changes in vegetation, it can be inferred that WPE has led to limestone porosity gains of approximately 0.1

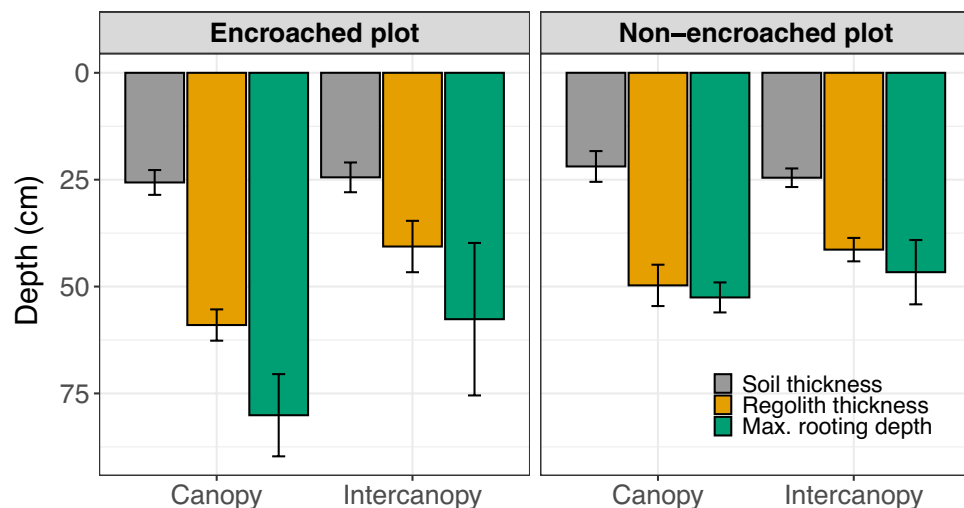


Figure 4. Bar graphs showing mean values of soil thickness (depth to the Cr1 layer), regolith thickness (depth to the Cr2 layer), and the maximum observed rooting depth by cover type (canopy vs. intercanopy) for the encroached and non-encroached sites. Error bars represent the 95% confidence interval.

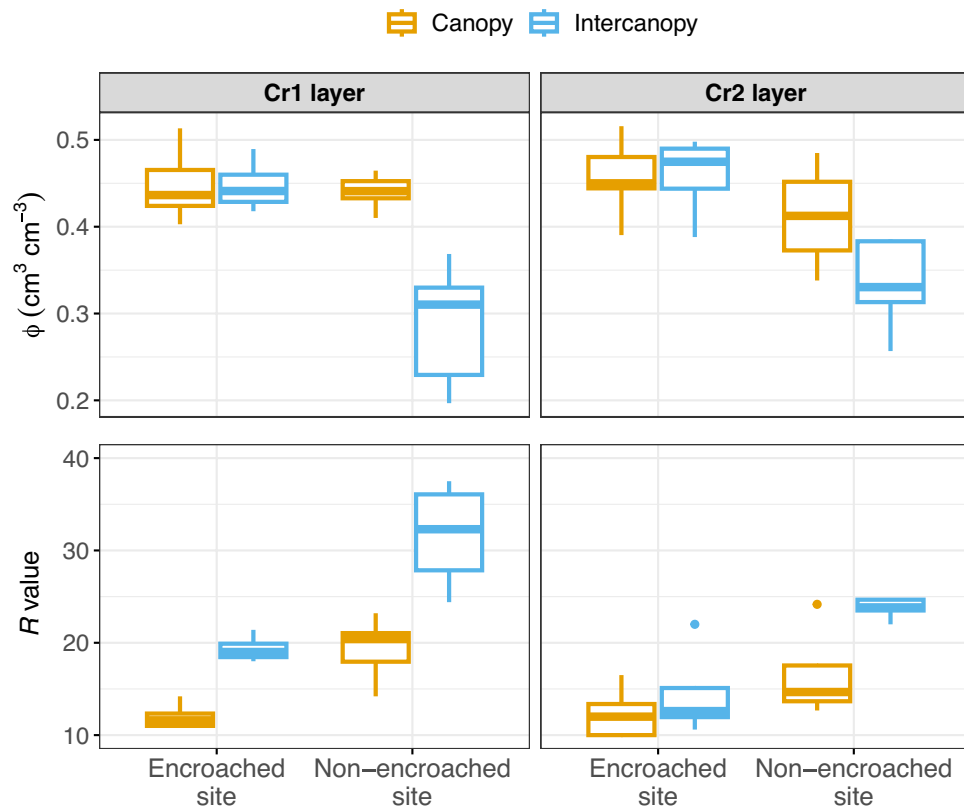


Figure 5. Box plots showing matrix porosity (Φ) and rebound values (R) of rock samples (obtained in situ with a Schmidt hammer) from the Cr1 and Cr2 layers of the encroached and non-encroached sites, by cover type (canopy vs. intercanopy).

$\text{cm}^3 \text{cm}^{-3}$ in less than a century. This finding contrasts starkly with the much slower rates of natural weathering of limestone, which would typically be on the order of several 1000 years for a comparable level of weathering to be reached⁴⁴. Compared with grasslands, woodlands add more organic matter to the soil and have greater root respiration rates—two processes that increase concentrations of dissolved CO_2 and organic acids in the vadose zone^{27,45} and ultimately promote chemical weathering and thereby increase porosity.

The porosity gains documented in our study are substantially higher than those reported by Wen et al. (2021) for encroached and non-encroached sites in the Konza Prairie in Kansas, USA²⁶. Using weathering models and stream solute concentrations, they estimated that it would take 300 years for WPE to result in a porosity gain of $0.01 \text{ cm}^3 \text{cm}^{-3}$. It is important to note that weathering rates can vary with environmental conditions, geological settings, and bedrock characteristics. Our findings, while limited to two trenches, provide novel field evidence of substantial and relatively short-term bedrock weathering by encroaching woody plants. Additional investigations in other karst regions undergoing WPE are needed to determine whether our findings apply to other locations.

Woody plants can enhance bedrock permeability through various mechanisms. Field evidence suggests that an important mechanism by which woody plants can enhance bedrock permeability is biomechanical root action, which creates preferential flow paths. Trench observations indicated that the canopy zones had a significantly thicker Cr1 layer and both the Cr1 layer and the petrocalcic film between it and the Cr2 layer were visually more broken down than in intercanopy zones (Figs. 2 and 4; also, see the *Trenching and pedologic observations* section in *Methods*). Additionally, the Cr2 layer in canopy zones displayed more abundant fractures and conduits, as well as root channels that were visually larger and extended to significantly greater depths. While roots mainly grow into existing rock fractures or highly weathered joints, ectomycorrhizal fungi associated with roots of many woody plants can penetrate narrow micropores of the rock matrix^{46,47}. Some of these symbiotic microorganisms have been shown to promote biochemical weathering by excreting low-molecular-weight organic acids—earning them the name “rock-eating fungi”⁴⁸. In other words, the high K_{sat} under canopies (especially where K_{sat} values were orders of magnitude higher than in intercanopy zones) is largely due to preferential flow through these features. Similar observations have been made by other researchers, who found that despite occupying less than 2% of the pore space, root channels contributed 93% of the saturated hydraulic conductivity of a weathered saprolite¹⁹. In addition to direct root action, woody plants might indirectly promote preferential flow by facilitating faunal activity. Biopores (e.g., termite tunnels) were visibly more abundant under trees (Fig. 2f). Invertebrate bioturbation can contribute to the high soil infiltration rates under woody plants^{49,50}, and this might also be the case for bedrock permeability.

Chemical weathering, by increasing matrix porosity, likely contributed to the enhancement of permeability rates. However, a paradox emerges in the case of the intercanopy zone of the encroached site: permeability remains comparatively low despite the fact that matrix porosity is as high as that found in the canopy zone (a feature we attribute to the dense woody plant cover surrounding the intercanopy). An indirect explanation for this reduced permeability could be the greater rock hardness in the intercanopy of both the encroached and non-encroached sites—as supported by our observation of generally higher R values in these zones (Fig. 5). Greater rock hardness means more resistance to root penetration and thereby lessened development of preferential flow paths via biomechanical weathering. Thus, while enhanced matrix porosity can contribute to increased permeability, if rock strength is high enough to restrict root-mediated biomechanical weathering, that factor might play a more pivotal role.

Another indirect way in which trees can promote chemical weathering and limestone permeability is by increasing soil infiltration capacity. When infiltration rates are higher and overland flow is lower, more water can reach the underlying limestone. At the Sonora Station, water has been shown to infiltrate five times faster and reach three times greater depths under junipers than in intercanopy soils⁵. As reactive water infiltrates deep through root channels and enlarged fissures, it accelerates carbonate dissolution and deepens the weathering front^{20,26}. Over time, more roots can penetrate the increasingly weathered rock, and the process becomes mutually reinforcing^{24,51}.

The enhanced bedrock permeability brought about by woody plants has ecohydrological implications. In this study, we examined the extent to which WPE might have accelerated weathering of carbonate parent material in a semiarid climate. These observations, in combination with those from previous studies documenting changes in soil infiltrability following WPE^{5,52,53} provide strong evidence that WPE appreciably alters soils and substrates in karst terrain. These changes can have important implications for ecohydrological dynamics in these landscapes—in particular because they have the potential to modify (1) subsurface lateral flows, (2) deep percolation, and (3) groundwater recharge. Below we present support for these assertions.

Subsurface lateral flow. In semiarid regions, the main runoff process is generally considered to be infiltration-excess overland flow, which is controlled by the infiltrability of the topsoil⁵⁴. However, where soils are shallow, bedrock permeability can also exert a strong control on runoff. If permeability is low, perched water tables can form, leading to saturation-excess overland flow and shallow subsurface lateral flow^{52,55}. Even when soils are unsaturated, high-intensity storms can generate subsurface flow, as rapid preferential flow through soils encounters low-permeability bedrock^{52,56}.

High-intensity, hillslope-scale rainfall simulation experiments in the Edwards Plateau have demonstrated that shallow subsurface flow can be an important component of runoff generation in these landscapes, particularly under tree canopies^{52,53}. These simulations produced no surface runoff from canopy zones but did produce large amounts of fast lateral subsurface flow through bedrock fractures filled with woody roots. From intercanopy zones, in contrast, the simulations produced substantial surface runoff and little subsurface flow (most of the latter through the interface between soil and bedrock)^{52,53}. Our findings of higher rates of weathering and limestone permeability beneath woody plants provide a mechanistic explanation for the results of those simulation experiments, showing that trees can create preferential flow networks in weathered bedrock and thereby promote shallow subsurface lateral flows.

Deep percolation. The acceleration of weathering and promotion of preferential flows brought about by WPE will likely contribute to deep percolation within the root zone. For example, continuous measurements of rock moisture at our study site showed that following a 95-mm storm event, the water content of fractures in the Cr2 layer (at 60 cm and 80 cm deep) peaked within 2–3 h of peak rainfall. At the same depths, the water content of the unfractured limestone matrix would take days or even weeks to show changes⁵⁷. Further evidence that woody plants can promote deep percolation comes from observations of trees channeling large amounts of water deep into the bedrock vadose zone via a combination of stemflow and preferential flow along fractures and root channels^{58,59}.

By enhancing the recharge of deeper water pools within the root zone, trees might increase their chances for long-term survival. For example, work in the Edwards Plateau has shown that juniper and oak trees on shallow soils underlain by fractured bedrock have lower mortality rates than those on deep soils⁶⁰—evidence not only of their ability to use rock moisture, but that it is a valuable resource for maintaining basic physiological functions during dry periods^{14,22,61}. We postulate that these plants' ability to also alter bedrock within their lifetime will favor both their survival rates and overall fitness—a clear example of niche construction⁶². When bedrock is permeable and porous, which facilitates deep water percolation and high available water storage, woody plants' competition with shallower-rooted grasses might be reduced. Young seedlings are more affected by this competition⁶³ and could reap the most benefit, as their survival rates improve when they have access to bedrock heterogeneities such as fissures and joints^{25,34}. Contrary to soil modifications, which may have relatively short-lived geomorphological signatures, rock weathering is irreversible and persists long after woody plants have died or been removed—an illustration of ecosystem engineering^{24,64}.

Groundwater recharge. Where bedrock permeability is high, vertical flows can be intensified, facilitating deep drainage and opportunities for direct groundwater recharge. Multiple factors govern these processes, including climate, geological setting, rooting depths, and depth to the water table^{2,65}. In semiarid karst settings, recharge occurs mainly following high-intensity storms, when water bypasses much of the vadose zone via preferential

flow⁶⁶. However, if most of the infiltrated water is stored within the root zone and transpired by vegetation, direct recharge will be minimal^{65,67}.

While direct recharge might be negligible in many semiarid regions, focused recharge in topographic depressions and karst features can be substantial^{55,68}. In this context, the effects of higher bedrock permeability and porosity brought about by WPE can be complex and hard to predict. Increased bedrock permeability could help explain the high levels of subsurface lateral flow observed under woody plants⁵². Such flows can bypass much of the soil and rock matrix^{57,58} and drain into ephemeral springs and streams, where recharge occurs via transmission losses⁶⁸. Alternatively, higher bedrock permeability and porosity could result in more water being stored on-site and being transpired instead of becoming runoff, consequently lowering focused recharge.

Conclusion

Our study provides evidence of the profound impact of WPE on the hydraulic properties of carbonate bedrock. Through biomechanical root action and biochemical processes, woody plants create preferential flow networks in weathered bedrock. This altered subsurface hydrology has important implications for ecohydrological dynamics, potentially affecting subsurface lateral flows, deep percolation, and groundwater recharge. As WPE continues to shape landscapes, understanding its effects on bedrock permeability and water pathways becomes increasingly important for managing water resources in semiarid ecosystems, particularly those with shallow soils. Further research is warranted to explore the interplay between WPE, bedrock weathering, and water dynamics across diverse climatic and geological settings.

Methods

Trenching and pedologic observations. To investigate the nature of the limestone bedrock, we excavated two trenches, one in each site (by means of a backhoe with a 90-cm-wide excavator bucket). We selected the trenching method because it is cost-effective and allowed us to not only take samples but also collect in situ data on rock hardness, depth to different horizons, and rooting depths. The trenches also enabled us to confirm that both plots were on the same continuous bed. In the encroached site, the trench was 16 m long, 11 m of which traversed a canopy zone and 5 m traversed an intercanopy zone. In the non-encroached site, the trench was 15 m long—5 m traversing the canopy of the Live oak tree and 10 m traversing intercanopy (Fig. 1). Whereas the encroached site trench was relatively easy to excavate to a depth of 1.5 m, the limestone beneath the non-encroached site was considerably harder to excavate, particularly in the intercanopy zone. The maximum depth attained in the non-encroached-site trench was 1 m, and only a 10-m-long section was deeper than 50 cm. That section was used for our rock sampling and analysis (described below).

In both trenches, three major layers could be easily distinguished: soil, a highly fractured and broken limestone layer (Cr1 layer), and a much less fractured limestone layer (Cr2 layer) (Fig. 2). Soils are very shallow Calciustolls, consisting of an A horizon (5–15 cm thick) of dark brown, silty clay loam and a Bw horizon (5–15 cm thick) of brown clay containing more than 50% rounded limestone cobbles and stones. Along with woody plant roots, most of the non-woody roots (from grasses, forbs, and cacti) were found in the A horizon. Woody roots were also abundant in the Bw horizon and in the weathered limestone. The Cr1 layer is 20–40 cm thick and consists of highly fractured and moderately hard limestone. In canopy zones, this layer was visibly more broken down, had wider fractures and conduits (often infilled with soil), and had thicker and more plentiful woody roots (Fig. 2b) than in intercanopy zones (Fig. 2a). The Cr2 layer consists of moderately soft to hard limestone with far fewer fractures and woody roots than the Cr1 layer. In canopy zones, the Cr2 layer was relatively soft and friable (fragments easily broken by hand), with medium-size woody roots growing both in fractures and directly through the matrix (Fig. 2c); in intercanopy zones, the Cr2 layer was harder (not easily broken by hand), with fewer and thinner woody roots, mostly growing in narrow fractures. This layer also exhibited occasional widened fractures and conduits infilled with soil and containing many woody roots, more commonly in canopy zones (Fig. 2e). Faunal biopores (e.g., termite tunnels) were observed in both weathered limestone layers but were clearly more abundant underneath trees (Fig. 2f). The boundary between the two layers was identified as a thin film of very hard limestone believed to have a pedogenic (petrocalcic) origin—formed by the dissolution and transport of carbonates from the soil and Cr1 layers and subsequent reprecipitation onto the less permeable Cr2 layer⁶⁹. This thin film was generally broken down, especially in canopy zones (Fig. 2d).

Limestone permeability. In August 2020, we drilled a total of 25 boreholes within each plot, using a compressed-air rock drill (Ingersoll-Rand, Piscataway, NJ, USA) with a 7.62-cm-diameter bit. The boreholes were drilled to the full reach of the drill (61 cm), at the nodes of a grid with 5-m spacing (Fig. 1), and each succeeded in attaining weathered bedrock. The boreholes were then cleaned—first by manual removal of large debris, then with a planer auger to remove finer debris and level the bottom, and finally with a leaf blower having an extended nozzle to remove dust and very fine debris. Boreholes located under woody plants were classified as “canopy,” and those located in open spaces (i.e., no tree cover) as “intercanopy”.

We used saturated hydraulic conductivity (K_{sat}) as our metric for weathered bedrock permeability. To ensure continuous and automatic measurement in the field, we used constant-head well permeameters (Supplementary materials; Figure S1). These permeameters are widely employed for measuring the permeability of soils and weathered parent material^{70,71}. Because water ponds inside the well, the infiltration process tends to be controlled by preferential flow through empty root channels, conduits, and fractures¹⁸. Thus, K_{sat} data obtained via well permeameter methods are particularly useful for evaluating changes in macrostructure⁷², such as mechanical weathering. We opted to use a relatively small (5-cm) head to ensure that measurements were performed within the weathered bedrock, which was confirmed by visual inspections. However, from the boreholes it was difficult

to distinguish between the Cr1 and Cr2 layers, and some tests likely included a combination of the two, which might have contributed to some of the large variability in K_{sat} .

During operation, changes in gas pressure in the permeameter were monitored by a datalogger and recorded every 30 s (Figure S2). The change in the permeameter's water level and gas pressure are related as follows:

$$\Delta P_g = -pg \Delta h \quad (1)$$

where ΔP_g is the change in gas pressure in the permeameter, p is the density of water, g is the acceleration of gravity, and Δh is the water head drop in the permeameter. Thus, the steady-state flow rate (Q) can be obtained by

$$Q = \Delta P_g (r^2) \pi / pg \Delta t \quad (2)$$

where r is the radius of the reservoir and Δt is the change in time (Figure S2).

Then, K_{sat} can be calculated as

$$K_{sat} = CQ / \left(2\pi H^2 + \pi a^2 C + \frac{2\pi H}{\alpha^*} \right) \quad (3)$$

where H is the ponded water head in the well, a is the well radius, α^* is a capillary length factor dependent on texture–structure category, and C is the shape coefficient, calculated as

$$C = \left[\left(\frac{H}{a} \right) / \left(Z_1 + Z_2 \left(\frac{H}{a} \right) \right) \right]^{Z_3} \quad (4)$$

where Z_1 , Z_2 , and Z_3 are empirically determined constants that depend on the α^* value. Since the precise value of α^* was not known, we used an estimated value of 0.01 cm^{-1} , which is suitable for mediums with very strong capillarity⁷¹. Although this approximation may introduce uncertainty in the absolute K_{sat} values, the relative differences in K_{sat} remain unaffected and valid regardless of the selected α^* value.

Measurements were terminated after the permeameter was entirely evacuated, or—in cases when infiltration was particularly slow—after at least 2 h of monitoring. While early termination of tests could have resulted in K_{sat} overestimation, the infiltration curves (e.g., Figure S2) indicated that steady-state was always achieved.

Other properties of limestone. In each of the two trenches, at 50-cm intervals, we recorded the depth to the Cr1 layer (soil thickness), the depth to the Cr2 layer (regolith thickness), and the deepest woody root observed (Figure S6). To estimate the hardness of the limestone surface, we performed in situ measurements of rebound values (R) using an H-2975 Schmidt hammer device (Humboldt Scientific, Raleigh, NC). This device measures the rebound of a spring-loaded metal piston hitting a surface at a defined energy. It has been used extensively in geomorphological studies, which have shown that the R values directly reflect the surface hardness of the rock and are highly correlated with rock compressive strength and degree of weathering⁷³. Before performing a test, we smoothed the rock surface with a medium-grained grinding stone. Then, at each point selected for later collection of a rock sample, we carried out the tests—at a right angle to the flat surface and avoiding visible fractures. We took five to six measurements at each point and averaged the resulting R values.

Next, we took cobble-size samples of the Cr1 and Cr2 layers at 1-m intervals. Samples from the Cr1 layer were taken from the middle of the layer, while samples from the Cr2 layer were taken at a depth of 20 cm below the top of the layer (Figure S6). In the laboratory, a piece of thread seal tape was tied around the samples, which were placed in a water container and left there for 48 h to achieve saturation. Then, while hanging from the tape, the samples were submerged one by one in a water-filled container mounted on top of a precision scale (0.01-g resolution), and the weight change was recorded. Because the change in weight is equivalent to the volume of water displaced by the sample (i.e., water density $\cong 1 \text{ g cm}^{-3}$), the sample's volume (V [cm^3]) can be readily obtained with an accuracy of 0.01%—the same level of accuracy as that of pycnometers⁷⁴. Finally, we calculated dry bulk density (ρ_b [g cm^{-3}]) and matrix porosity (Φ [$\text{cm}^3 \text{ cm}^{-3}$]), respectively, as follows:

$$\rho_b = \frac{m_{dry}}{V} \quad (5)$$

$$\Phi = \left(1 - \frac{\rho_b}{\rho_s} \right) \quad (6)$$

Where m_{dry} is the dry mass (obtained by oven drying the sample at $105 \text{ }^\circ\text{C}$ for 48 h) and ρ_s is the particle density of limestone, for which the value of 2.66 g cm^{-3} was adopted⁷⁵.

Statistical analyses. To test the null hypothesis of no significant differences among the groups and no interaction effect, we performed a two-way ANOVA to evaluate the significance of (1) effects of the predictor variables *cover* (canopy vs. intercanopy) and *site* (encroached vs. non-encroached), and (2) the effect of their interaction on the response variable. This procedure was adopted for data conforming to parametric assumptions (log10-transformed K_{sat} , depth to Cr1, depth to Cr2, and maximum rooting depth). Even after various transformations, the porosity and R values did not conform to assumptions of normality and equal variance, and for this reason we used the non-parametric Mann–Whitney test to identify significant differences between median values. All analyses were performed in R version 4.1.0. with a significance level of 0.05. To visualize the

spatial trends of K_{sat} at the plot scale, we created 2-d interpolation maps using the loess() function of the R package 'stats'.

Data availability

The datasets generated and/or analyzed during the current study are available as Supplementary information files.

Received: 3 March 2023; Accepted: 7 September 2023

Published online: 18 September 2023

References

1. Archer, S. R. *et al.* Woody plant encroachment: Causes and consequences. In *Rangeland Systems: Processes, Management and Challenges* (ed. Briske, D. D.) 25–84 (Springer International Publishing, Cham, 2017). https://doi.org/10.1007/978-3-319-46709-2_2.
2. Wilcox, B. P., Basant, S., Olariu, H. & Leite, P. A. M. Ecohydrological connectivity: a unifying framework for understanding how woody plant encroachment alters the water cycle in drylands. *Front. Environ. Sci.* **10**, 934535 (2022).
3. Ilstedt, U. *et al.* Intermediate tree cover can maximize groundwater recharge in the seasonally dry tropics. *Sci. Rep.* **6**, 21930 (2016).
4. Basant, S., Wilcox, B. P., Leite, P. A. & Morgan, C. When savannas recover from overgrazing, ecohydrological connectivity collapses. *Environ. Res. Lett.* <https://doi.org/10.1088/1748-9326/ab71a1> (2020).
5. Leite, P. A. M., Wilcox, B. P. & McInnes, K. J. Woody plant encroachment enhances soil infiltrability of a semiarid karst savanna. *Environ. Res. Commun.* **2**, 115005 (2020).
6. Eldridge, D. J. & Freudenberger, D. Ecosystem wicks: Woodland trees enhance water infiltration in a fragmented agricultural landscape in eastern Australia. *Austral Ecol.* **30**(3), 336–347. <https://doi.org/10.1111/j.1442-9993.2005.01478.x> (2005).
7. Liu, Y.-F. *et al.* Shrub encroachment enhances the infiltration capacity of alpine meadows by changing the community composition and soil conditions. *CATENA* **213**, 106222 (2022).
8. Zou, C. B., Turton, D. J., Will, R. E., Engle, D. M. & Fuhlendorf, S. D. Alteration of hydrological processes and streamflow with juniper (*Juniperus virginiana*) encroachment in a mesic grassland catchment: Alteration of hydrological processes after juniper encroachment. *Hydrol. Processes* **28**(26), 6173–6182. <https://doi.org/10.1002/hyp.10102> (2014).
9. Soliveres, S. & Eldridge, D. J. Do changes in grazing pressure and the degree of shrub encroachment alter the effects of individual shrubs on understory plant communities and soil function?. *Funct. Ecol.* **28**(2), 530–537. <https://doi.org/10.1111/1365-2435.12196> (2014).
10. Wilcox, B. P. & Huang, Y. Woody plant encroachment paradox: rivers rebound as degraded grasslands convert to woodlands. *Geophys. Res. Lett.* **37**, n/a–n/a (2010).
11. Schreiner-McGraw, A. P. *et al.* Woody plant encroachment has a larger impact than climate change on dryland water budgets. *Sci. Rep.* **10**, 8112 (2020).
12. McCormick, E. L. *et al.* Widespread woody plant use of water stored in bedrock. *Nature* **597**(7875), 225–229. <https://doi.org/10.1038/s41586-021-03761-3> (2021).
13. Rempe, D. M. & Dietrich, W. E. Direct observations of rock moisture, a hidden component of the hydrologic cycle. *Proc. Natl. Acad. Sci.* **115**(11), 2664–2669. <https://doi.org/10.1073/pnas.1800141115> (2018).
14. Hubbert, K. R., Graham, R. C. & Anderson, M. A. Soil and weathered bedrock: Components of a Jeffrey pine plantation substrate. *Soil Sci. Soc. Am. J.* **65**(4), 1255–1262. <https://doi.org/10.2136/sssaj2001.6541255x> (2001).
15. Jones, D. P. & Graham, R. C. Water-holding characteristics of weathered granitic rock in chaparral and forest ecosystems. *Soil Sci. Soc. Am. J.* **57**(1), 256–261. <https://doi.org/10.2136/sssaj1993.03615995005700010044x> (1993).
16. Worthington, S. R. H., Davies, G. J. & Calvin Alexander, E. Enhancement of bedrock permeability by weathering. *Earth-Sci. Rev.* **160**, 188–202. <https://doi.org/10.1016/j.earscirev.2016.07.002> (2016).
17. Graham, R., Rossi, A. & Hubbert, R. Rock to regolith conversion: Producing hospitable substrates for terrestrial ecosystems. *GSA Today* <https://doi.org/10.1130/GSAT57A.1> (2010).
18. Graham, R. C., Anderson, M. A., Sternberg, P. D., Tice, K. R. & Schoeneberger, P. J. Morphology, porosity, and hydraulic conductivity of weathered granitic bedrock and overlying soils. *Soil Sci. Soc. Am. J.* **61**, 516 (1997).
19. Vepraskas, M. J., Hoover, M. T., Jongmans, A. G. & Bouma, J. Hydraulic conductivity of saprolite as determined by channels and porous groundmass. *Soil Sci. Soc. Am. J.* **55**(4), 932–938. <https://doi.org/10.2136/sssaj1991.03615995005500040006x> (1991).
20. Brantley, S. L. *et al.* Reviews and syntheses: On the roles trees play in building and plumbing the critical zone. *Biogeosciences* **14**(22), 5115–5142. <https://doi.org/10.5194/bg-14-5115-2017> (2017).
21. Tune, A. K., Druhan, J. L., Wang, J., Bennett, P. C. & Rempe, D. M. Carbon dioxide production in bedrock beneath soils substantially contributes to forest carbon cycling. *J. Geophys. Res. Biogeosci.* <https://doi.org/10.1029/2020JG005795> (2020).
22. Sternberg, P. D., Anderson, M. A., Graham, R. C., Beyers, J. L. & Tice, K. R. Root distribution and seasonal water status in weathered granitic bedrock under chaparral. *Geoderma* **72**(1–2), 89–98. [https://doi.org/10.1016/0016-7061\(96\)00019-5](https://doi.org/10.1016/0016-7061(96)00019-5) (1996).
23. Graham, R. C., Tice, K. R. & Guertal, W. R. The pedologic nature of weathered rock. In *Whole Regolith Pedology* (eds Cremeens, D. L. *et al.*) 21–40 (Soil Science Society of America, Madison, WI, USA, 1994). <https://doi.org/10.2136/sssaspecpub34.c2>.
24. Pawlik, Ł., Phillips, J. D. & Šamonil, P. Roots, rock, and regolith: Biomechanical and biochemical weathering by trees and its impact on hillslopes—A critical literature review. *Earth-Sci. Rev.* **159**, 142–159. <https://doi.org/10.1016/j.earscirev.2016.06.002> (2016).
25. Phillips, J. D., Turkington, A. V. & Marion, D. A. Weathering and vegetation effects in early stages of soil formation. *Catena* **72**(1), 21–28. <https://doi.org/10.1016/j.catena.2007.03.020> (2008).
26. Wen, H., Sullivan, P. L., Macpherson, G. L., Billings, S. A. & Li, L. Deepening roots can enhance carbonate weathering by amplifying CO₂-rich recharge. *Biogeosciences* **18**(1), 55–75. <https://doi.org/10.5194/bg-18-55-2021> (2021).
27. Sullivan, P. L. *et al.* How landscape heterogeneity governs stream water concentration-discharge behavior in carbonate terrains (Konza Prairie, USA). *Chem. Geol.* **527**, 118989 (2019).
28. Macpherson, G. L. & Sullivan, P. L. Watershed-scale chemical weathering in a merokarst terrain, northeastern Kansas, USA. *Chem. Geol.* **527**, 118988 (2019).
29. Macpherson, G. L., Sullivan, P. L., Stotler, R. L. & Norwood, B. S. Increasing groundwater CO₂ in a mid-continent tallgrass prairie: Controlling factors. in *E3S Web of Conferences* vol. 98 06008 (EDP Sciences, 2019).
30. Western Regional Climate Center. <https://wrcc.dri.edu> (Accessed on 17 Aug 2021).
31. Cleveland, T. G. *et al.* *New rainfall coefficients: Including tools for estimation of intensity and hyetographs in Texas*. No. FHWA/TX-15/0-6824-1. Texas. Dept. of Transportation. Research and Technology Implementation Office (2015).
32. Smeins, F. E., Fuhlendorf, S. D. & Taylor, C. A. Environmental and land use changes: A long-term perspective. in *Juniper Symposium 1* (Texas A&M Research and Extension Center, 1997).
33. Long, A. T. *Ground Water Geology of Edwards County Texas*, No. 1619-J (US Geological Survey, 1963).
34. Gabet, E. J. & Mudd, S. M. Bedrock erosion by root fracture and tree throw: A coupled geomorphic model to explore the humped soil production function and the persistence of hillslope soils. *J. Geophys. Res.* **115**, F04005 (2010).

35. Woodruff, C. M. & Wilding, L. P. Bedrock, soils, and hillslope hydrology in the Central Texas Hill Country, USA: Implications on environmental management in a carbonate-rock terrain. *Environ. Geol.* **55**(3), 605–618. <https://doi.org/10.1007/s00254-007-1011-4> (2007).
36. Wilcox, B. P., Wilding, L. P. & Woodruff, C. M. Soil and topographic controls on runoff generation from stepped landforms in the Edwards Plateau of Central Texas. *Geophys. Res. Lett.* **34**, L24S24 (2007).
37. Hassler, S. K., Zimmermann, B., van Breugel, M., Hall, J. S. & Elsenbeer, H. Recovery of saturated hydraulic conductivity under secondary succession on former pasture in the humid tropics. *For. Ecol. Manag.* **261**(10), 1634–1642. <https://doi.org/10.1016/j.foreco.2010.06.031> (2011).
38. Leite, P. A. M. *et al.* The influence of forest regrowth on soil hydraulic properties and erosion in a semiarid region of Brazil. *Ecohydrology* **11**, e1910 (2018).
39. Rolo, V. & Moreno, G. Interspecific competition induces asymmetrical rooting profile adjustments in shrub-encroached open oak woodlands. *Trees* **26**(3), 997–1006. <https://doi.org/10.1007/s00468-012-0677-8> (2012).
40. Cui, Z., Ze Huang, Y., Liu, M.L.-V. & Gao-Lin, W. Natural compensation mechanism of soil water infiltration through decayed roots in semi-arid vegetation species. *Sci. Total Environ.* **819**, 151985. <https://doi.org/10.1016/j.scitotenv.2021.151985> (2022).
41. Dammeyer, H. C., Schwinning, S., Schwartz, B. F. & Moore, G. W. Effects of juniper removal and rainfall variation on tree transpiration in a semi-arid karst: evidence of complex water storage dynamics: Effects of Juniper Removal in Karst. *Hydrol. Processes* **30**(24), 4568–4581. <https://doi.org/10.1002/hyp.10938> (2016).
42. Hayes, J. L., Riebe, C. S., Holbrook, W. S., Flinchum, B. A. & Hartsough, P. C. Porosity production in weathered rock: Where volumetric strain dominates over chemical mass loss. *Sci. Adv.* **5**, 0834 (2019).
43. Crowther, J. Ecological observations in tropical Karst Terrain, West Malaysia. III. Dynamics of the vegetation-soil-bedrock system. *J. Biogeogr.* **14**(2), 157. <https://doi.org/10.2307/2845069> (1987).
44. Dong, X. *et al.* Ecohydrologic processes and soil thickness feedbacks control limestone-weathering rates in a karst landscape. *Chem. Geol.* **527**, 118774 (2019).
45. Billings, S. A. *et al.* Loss of deep roots limits biogenic agents of soil development that are only partially restored by decades of forest regeneration. *Elementa Sci. Anthropocene* <https://doi.org/10.1525/elementa.287> (2018).
46. Bornyasz, M. A., Graham, R. C. & Allen, M. F. Ectomycorrhizae in a soil-weathered granitic bedrock regolith: Linking matrix resources to plants. *Geoderma* **126**(1–2), 141–160. <https://doi.org/10.1016/j.geoderma.2004.11.023> (2005).
47. Schwinning, S. The ecohydrology of roots in rocks. *Ecohydrology* **3**, 238–245. <https://doi.org/10.1002/eco.134> (2010).
48. Jongmans, A. G. *et al.* Rock-eating fungi. *Nature* **389**(6652), 682–683. <https://doi.org/10.1038/39493> (1997).
49. Marquart, A., Eldridge, D. J., Geissler, K., Lobas, C. & Blaum, N. Interconnected effects of shrubs, invertebrate-derived macropores and soil texture on water infiltration in a semi-arid savanna rangeland. *Land Degrad. Dev.* **31**, 2307–2318. <https://doi.org/10.1002/ldr.3598> (2020).
50. Leite, P. A. M., Carvalho, M. C. & Wilcox, B. P. Good ant, bad ant? Soil engineering by ants in the Brazilian Caatinga differs by species. *Geoderma* **323**, 65–73. <https://doi.org/10.1016/j.geoderma.2018.02.040> (2018).
51. Estrada-Medina, H., Graham, R. C., Allen, M. F., Jiménez-Osornio, J. J. & Robles-Casolco, S. The importance of limestone bedrock and dissolution karst features on tree root distribution in northern Yucatán, México. *Plant Soil* **362**(1–2), 37–50. <https://doi.org/10.1007/s11104-012-1175-x> (2012).
52. Wilcox, B. P. *et al.* Subsurface stormflow is important in semiarid karst shrublands: Subsurface stormflow and karst shrubland. *Geophys. Res. Lett.* <https://doi.org/10.1029/2008GL033696> (2008).
53. Taucer, P. I., Munster, C. L., Wilcox, B. P., Owens, M. K. & Mohanty, B. P. Large-scale rainfall simulation experiments on juniper rangelands. *Trans. ASABE* **51**(6), 1951–1961. <https://doi.org/10.13031/2013.25400> (2008).
54. Kidron, G. J. Comparing overland flow processes between semiarid and humid regions: Does saturation overland flow take place in semiarid regions?. *J. Hydrol.* **593**, 125624. <https://doi.org/10.1016/j.jhydrol.2020.125624> (2020).
55. Schreiner-McGraw, A. P. & Vivoni, E. R. On the sensitivity of hillslope runoff and channel transmission losses in arid piedmont slopes. *Water Resour. Res.* **54**(7), 4498–4518. <https://doi.org/10.1029/2018WR022842> (2018).
56. McKay, L. D., Driese, S. G., Smith, K. H. & Vepraskas, M. J. Hydrogeology and pedology of saprolite formed from sedimentary rock, eastern Tennessee, USA. *Geoderma* **126**, 27–45 (2005).
57. Leite, P. A. M., Wilcox, B. P., McInnes, K. J. & Walker, J. W. Applicability of soil moisture sensors for monitoring water dynamics in rock: A field test in weathered limestone. *Vadose Zone J.* <https://doi.org/10.1002/vzj2.20164> (2021).
58. Dasgupta, S., Mohanty, B. P., Knes, K. J. & Walker, J. W. Applicability of soil moisture sensors for monitoring water dynamics in rock. *Vadose Zone J.* **5**
59. Sassen, D. S., Everett, M. E. & Munster, C. L. Ecohydrogeophysics at the Edwards Aquifer: Insights from Polarimetric ground-penetrating radar. *Near Surf. Geophys.* **7**(5–6), 427–438. <https://doi.org/10.3997/1873-0604.2009032> (2009).
60. Crouchet, S. E., Jensen, J., Schwartz, B. F. & Schwinning, S. Tree mortality after a hot drought: Distinguishing density-dependent and -independent drivers and why it matters. *Front. For. Glob. Change* **2**, 21 (2019).
61. Schwinning, S. A critical question for the critical zone: How do plants use rock water?. *Plant Soil* **454**, 49–56 (2020).
62. John Odling-Smee, F., Laland, K. N. & Feldman, M. W. *Niche Construction: The Neglected Process in Evolution (MPB-37)* (Princeton University Press, 2013). <https://doi.org/10.1515/9781400847266>.
63. Kambatuku, J. R., Cramer, M. D. & Ward, D. Overlap in soil water sources of savanna woody seedlings and grasses. *Ecohydrology* **6**, 464–473 (2013).
64. Jones, C. G. Ecosystem engineers and geomorphological signatures in landscapes. *Geomorphology* **157–158**, 75–87 (2012).
65. Seyfried, M. S. *et al.* Ecohydrological control of deep drainage in arid and semiarid regions. *Ecology* **86**, 277–287 (2005).
66. Ries, F., Lange, J., Schmidt, S., Puhlmann, H. & Sauter, M. Recharge estimation and soil moisture dynamics in a Mediterranean, semi-arid karst region. *Hydrol. Earth Syst. Sci.* **19**(3), 1439–1456. <https://doi.org/10.5194/hess-19-1439-2015> (2015).
67. Heilman, J. L. *et al.* Water-storage capacity controls energy partitioning and water use in karst ecosystems on the Edwards Plateau, Texas: Water-storage controls water use in karst ecosystems. *Ecohydrology* **7**(1), 127–138. <https://doi.org/10.1002/eco.1327> (2014).
68. Green, R. T., Bertetti, F. P. & Miller, M. S. Focused groundwater flow in a carbonate aquifer in a semi-arid environment. *J. Hydrol.* **517**, 284–297 (2014).
69. Rabenhorst, M. C., West, L. T. & Wilding, L. P. Genesis of calcic and petrocalcic horizons in soils over carbonate rocks. In *Occurrence, Characteristics, and Genesis of Carbonate, Gypsum, and Silica Accumulations in Soils* (ed. Nettleton, W. D.) 61–74 (Soil Science Society of America, 1991). <https://doi.org/10.2136/sssaspecpub26.c4>.
70. Schoeneberger, P. J., Amoozegar, A. & Buol, S. W. Physical property variation of a soil and saprolite continuum at three geomorphic positions. *Soil Sci. Soc. Am. J.* **59**(5), 1389–1397. <https://doi.org/10.2136/sssaj1995.03615995005900050027x> (1995).
71. Elrick, D. E. & Daniel Reynolds, W. Infiltration from constant-head well permeameters and infiltrometers. In *Advances in Measurement of Soil Physical Properties: Bringing Theory into Practice* (eds Clarke Topp, G. *et al.*) 1–24 (Soil Science Society of America, 1992). <https://doi.org/10.2136/sssaspecpub30.c1>.
72. Elrick, D. E. & Reynolds, W. D. Methods for analyzing constant-head well permeameter data. *Soil Sci. Soc. Am. J.* **56**, 320 (1992).
73. Viles, H., Goudie, A., Grab, S. & Lallely, J. The use of the Schmidt Hammer and Equotip for rock hardness assessment in geomorphology and heritage science: A comparative analysis. *Earth Surf. Process. Landforms* **36**, 320–333 (2011).
74. Hughes, S. W. Archimedes revisited: A faster, better, cheaper method of accurately measuring the volume of small objects. *Phys. Educ.* **40**, 468–474 (2005).

75. Neville, A. M. *Properties of Concrete* (Pearson, UK, 2011).

Acknowledgements

This work was supported by the USDA-NIFA Grant 12726253, and P.A.M.L. was supported by the Texas A&M Sid Kyle and Tom Slick Graduate Fellowships. We would like to thank Fermin Saldivar and Matthew Rector for their help with the trench excavations and borehole drilling. We are also thankful to Doug Tolleson, Nick Garza, Robert Moen, and Ismael Sanchez for providing logistical support at the Texas A&M Sonora Station.

Author contributions

P.L. and L.S. conceptualized the study; B.W., K.M., J.W. and D.R. supervised and provided resources to P.L. and L.S.; P.L. and L.S. collected the data; P.L. analyzed the data and prepared the figures; H.O. performed vegetation cover analysis and prepared figures 1 and S3; P.L. wrote the main manuscript with substantial inputs from B.W., L.S., and D.R.; All authors reviewed the manuscript.

Competing interests

The authors declare no competing interests.

Additional information

Supplementary Information The online version contains supplementary material available at <https://doi.org/10.1038/s41598-023-42226-7>.

Correspondence and requests for materials should be addressed to P.A.M.L.

Reprints and permissions information is available at www.nature.com/reprints.

Publisher's note Springer Nature remains neutral with regard to jurisdictional claims in published maps and institutional affiliations.



Open Access This article is licensed under a Creative Commons Attribution 4.0 International License, which permits use, sharing, adaptation, distribution and reproduction in any medium or format, as long as you give appropriate credit to the original author(s) and the source, provide a link to the Creative Commons licence, and indicate if changes were made. The images or other third party material in this article are included in the article's Creative Commons licence, unless indicated otherwise in a credit line to the material. If material is not included in the article's Creative Commons licence and your intended use is not permitted by statutory regulation or exceeds the permitted use, you will need to obtain permission directly from the copyright holder. To view a copy of this licence, visit <http://creativecommons.org/licenses/by/4.0/>.

© The Author(s) 2023